Monthly Notices
of the
ROYAL ASTRONOMICAL SOCIETY

MNRAS **449,** 425–430 (2015) doi:10.1093/mnras/stv268

Alignment metrology for the Antarctica Kunlun Dark Universe Survey Telescope

Zhengyang Li,[1,2,3]* Xiangyan Yuan[1,2] and Xiangqun Cui[1,2]

[1]*National Astronomical Observatories/Nanjing Institute of Astronomical Optics and Technology, Chinese Academy of Sciences, Nanjing 210042, China*
[2]*Key Laboratory of Astronomical Optics and Technology, Nanjing Institute of Astronomical Optics and Technology, Chinese Academy of Sciences, Nanjing 210042, China*
[3]*University of Chinese Academy of Sciences, Beijing 100049, China*

Accepted 2015 February 8. Received 2015 February 8; in original form 2014 April 20

ABSTRACT

Dome A is the highest point on the Antarctic Plateau, and the Chinese expedition team was the first to arrive there in 2005 January. It is an excellent site for astronomical observations. The Kunlun Dark Universe Survey Telescope (KDUST), a proposed next-generation Chinese Antarctic optical telescope, is currently being planned. KDUST is a coaxial three-mirror anastigmatic telescope with an entrance pupil diameter of 2.5 m and a field of view of $1^{\circ}.5$. The telescope should be fully aligned in order to achieve diffraction-limited image quality. Based on the current optical model for KDUST, in this study we describe a modified alignment metrology and give the preliminary results of numerical simulations. Using the acquisition of field-dependent aberrations, the algorithm, which is based on double Zernike polynomial decomposition and the least-squares fitting method, delivers a suitable set of corrections for resolving misalignments including the multi-axis motion of the secondary and tertiary mirrors. Moreover, the algorithm can also be used to calculate the primary mirror's low-order figure errors mixing with the misalignments of the secondary mirror.

Key words: methods: miscellaneous – telescopes.

1 INTRODUCTION

The preliminary site testing performed since the beginning of 2008 shows that Antarctic Dome A is an excellent astronomical site for observing wavelengths ranging from visible to infrared and submillimetre (Yang et al. 2010). The Chinese Small Telescope Array (CSTAR) and the first Antarctic Survey Telescope (AST3-1) were mounted on Dome A in 20 d at an altitude of 4091 m and at a summer temperature of -40°C (Zhengyang, Xiangyan & Xiangqun 2012). Two other Antarctic Survey Telescopes are currently being developed and the 2.5-m KDUST is proposed for Dome A high-resolution observations. Although the assembly of the Antarctic telescopes has been modularized, the *in situ* telescope assembly and alignment is challenging work, especially for future diffraction-limited telescopes such as KDUST. In this study, an alignment metrology that utilizes aberration measurement and decomposition offers a possible method to calculate the misalignment value. Then, the *in situ* alignment tasks might be accomplished as same as laboratorial or factory alignment.

Generally, measured aberrations can be studied to scale or calculate misalignments. Hopkins (1950) improved the wave theory of aberration and developed a basic set of wavefront equations for rotationally symmetric optical systems. In 1970, Shack used a vector formulation to interpret the wavefront expansion, and Buchroeder (1976) introduced a vector σ to represent the centre shift of field-dependent aberrations due to a misaligned system. In the 1980s, nodal aberration theory (NAT), first reported by Shack & Thompson (1980), was used to explore the relationship between misalignments and field-dependent aberrations. According to NAT, the performance of a misaligned telescope is dominated by field uniform coma and field asymmetric field linear astigmatism (Thompson, Schmid & Rolland 2008; Thompson et al. 2009). Furthermore, the nodal behaviour of NAT can be directly revealed by Zernike polynomials, which are capable of characterizing the aberrations of optical systems. A 1.2-m Ritchey–Chrétien (R–C) telescope had been aligned by minimizing both coma (Z7/Z8) and astigmatism (Z5/Z6) across the field (Mcleod 1996).

Manuel (2009) introduced a basic set of orthogonal double Zernike polynomials (DZPs) over the pupil and the field, which are used to decompose aberrations in NAT. Moreover, Manuel applied the concept to iteratively solve the misalignment problems of the Hobby–Eberly telescope using the singular value decomposition (SVD) method. The misaligned aberrations of less sensitive elements are compensated by overcorrecting sensitive elements, the misalignments of which produce large-scale aberrations. So, the SVD solutions for the misalignments of less sensitive elements might not be as accurate as those of the more sensitive

* E-mail: zyli@niaot.ac.cn

elements. Therefore, in this study, we use the least-squares fitting (LSF) method to produce a high-quality solution for multi-element misalignments. Moreover, we are able to calculate the primary mirror's low-order figure errors mixing with secondary mirror misalignments.

2 DESCRIPTION OF NAT AND CHARACTERIZING NAT WITH DZPS

NAT is based on the wave aberration theory of Hopkins, combined with the insights of shifted aberration field centres and the discovery of the nodal behaviour of misaligned aberrations. A complete treatment of third-order NAT was accomplished by Thompson, as well as fifth-order aberrations including spherical aberration, coma and astigmatism.

The NAT wavefront expression for the misaligned optical system is given by

$$W(\boldsymbol{H},\boldsymbol{\rho}) = \sum_j \sum_{p=0}^{\infty}\sum_{n=0}^{\infty}\sum_{m=0}^{\infty}(W_{klm})\left[(\boldsymbol{H}-\boldsymbol{\sigma}_j)\bullet(\boldsymbol{H}-\boldsymbol{\sigma}_j)\right]^p \times(\boldsymbol{\rho}\bullet\boldsymbol{\rho})^n\left[(\boldsymbol{H}-\boldsymbol{\sigma}_j)\bullet\boldsymbol{\rho}\right]^m, \quad (1)$$

where W_{klm} is the aberration coefficient, $\boldsymbol{H}$ represents the normalized image field position, $\boldsymbol{\rho}$ is the normalized pupil position and $\boldsymbol{\sigma}_j$ denotes the aberration field centre shifting vector. The total wave aberration is the sum of j surface contributions. In rotationally symmetric optical systems, the coefficients satisfy the relations $k = 2p + m$ and $l = 2n + m$. Fig. 1 shows the conventions used in this paper.

Starting with equation (1), misaligned third-order aberrations, such as spherical aberration astigmatism and coma, can be written with the NAT concept as follows (Thompson 2005):

$$\begin{aligned} W_{\text{spheri}} &= W_{040}\,(\boldsymbol{\rho}\bullet\boldsymbol{\rho})^2;\\ W_{\text{astig}} &= \frac{1}{2}\left(W_{222}\boldsymbol{H}^2 - 2\boldsymbol{H}\boldsymbol{A}_{222} + \boldsymbol{B}_{222}^2\right)\bullet\rho^2;\\ W_{\text{coma}} &= \left[(W_{131}\boldsymbol{H}-\boldsymbol{A}_{131})\bullet\boldsymbol{\rho}\right]\bullet\rho^2. \end{aligned} \quad (2)$$

The vectors $\boldsymbol{A}$ and $\boldsymbol{B}$ are the sums of the surface contribution displacement vectors, which are defined as

$$\begin{aligned} \boldsymbol{A}_{131} &= \sum_j W_{131_j}\boldsymbol{\sigma}_j;\\ \boldsymbol{A}_{222} &= \sum_j W_{222_j}\boldsymbol{\sigma}_j;\\ \boldsymbol{B}_{222}^2 &= \sum_j W_{222_j}\boldsymbol{\sigma}_j^2. \end{aligned} \quad (3)$$

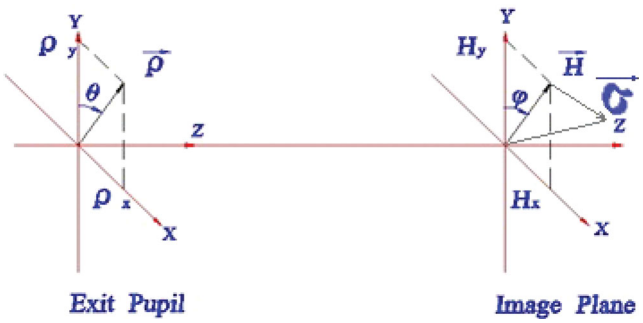

Figure 1. Conventions for field vector and pupil vector.

The vector formulation of the wavefront error expansion indicates that the spherical aberration is independent of the field, while the misaligned optical system performance is dominated by field uniform coma and field asymmetric field linear astigmatism. Therefore, the misaligned aberrations always have minimum points known as nodes in the image plane.

Based on third-order NAT, the procedure for correcting an arbitrary misalignment of an R−C telescope can be effectively determined. In case there are multiple surfaces, such as for the Large Synoptic Survey Telescope (LSST), an alignment plan based on NAT might need an additional fifth-order misaligned aberration, which is used to decouple the relationship between the aberration nodes and the motions of elements, known as degrees of freedom (d.o.f.; Sebag et al. 2012).

We believe a suitable numerical characterization of NAT can be achieved with the orthogonal DZPs introduced by Manuel (2009). An orthogonal set of DZP terms provides a decomposition that can be used with NAT, containing the field Zernike polynomials and pupil Zernike polynomials, which can directly reveal the misaligned field aberrations. In general, the field-dependent aberrations can be described with a set of four DZP functions to form a complete basis by applying of vector multiplication and polar coordinates, as follows (Manuel 2009):

$$\begin{aligned} S_A(h,\varphi,\rho,\theta) &= Z_k(h,\varphi)Z_i(\rho,\theta) + Z_l(h,\varphi)Z_j(\rho,\theta);\\ S_B(h,\varphi,\rho,\theta) &= Z_k(h,\varphi)Z_i(\rho,\theta) - Z_l(h,\varphi)Z_j(\rho,\theta);\\ S_C(h,\varphi,\rho,\theta) &= Z_l(h,\varphi)Z_j(\rho,\theta) + Z_k(h,\varphi)Z_i(\rho,\theta);\\ S_D(h,\varphi,\rho,\theta) &= Z_l(h,\varphi)Z_j(\rho,\theta) - Z_k(h,\varphi)Z_i(\rho,\theta). \end{aligned} \quad (4)$$

Here, S_A, S_B and S_C, S_D are orthogonal.

Consider the following example of the third NAT astigmatism:

$$\begin{aligned} W_{\text{astigmatism}}^{\text{quadratic}}(h,\varphi,\rho,\theta) &= \alpha_0[Z_5(h,\theta)Z_5(\rho,\phi)+Z_6(h,\theta)Z_6(\rho,\phi)];\\ W_{\text{astigmatism}}^{\text{linear}}(h,\theta,\rho,\phi) &= \alpha_1[Z_3(h,\theta)Z_5(\rho,\phi)+Z_2(h,\theta)Z_6(\rho,\phi)]\\ &\quad+\alpha_2[Z_2(h,\theta)Z_5(\rho,\phi)-Z_3(h,\theta)Z_6(\rho,\phi)];\\ W_{\text{astigmatism}}^{\text{const}}(h,\theta,\rho,\phi) &= \alpha_3 Z_1(h,\theta)Z_5(\rho,\phi)+\alpha_4 Z_1(h,\theta)Z_6(\rho,\phi). \end{aligned} \quad (5)$$

The Zernike polynomials discussed in the study are given in standard form in association with the ZEMAX software.

Therefore, the misaligned field aberrations can be described by DZP including the effects of the field dependence. When aligning a real telescope, we must modify the nominal design with optical shop testing results, and then consider the performance of the modified optical system as a fully aligned target. We individually perturb each d.o.f. by a unit value; we define the unit value for each d.o.f. in the next section and record the field aberrations as one pattern. In this way, the primary mirror astigmatic figure error can also be treated as a d.o.f. Finally, we measure the real misaligned system field aberrations and use the LSF method to solve the misalignments of each d.o.f. Based on these insights, the modelling alignment of KDUST described in the next section illustrates that the metrology is feasible and accurate.

3 APPLICATION OF THE ALIGNMENT METROLOGY TO ANTARCTICA KDUST

3.1 KDUST optical specification

The KDUST optical system is a coaxial three-mirror anastigmatic telescope (TMA) system with a 2.5-m F/1.06 primary mirror. The

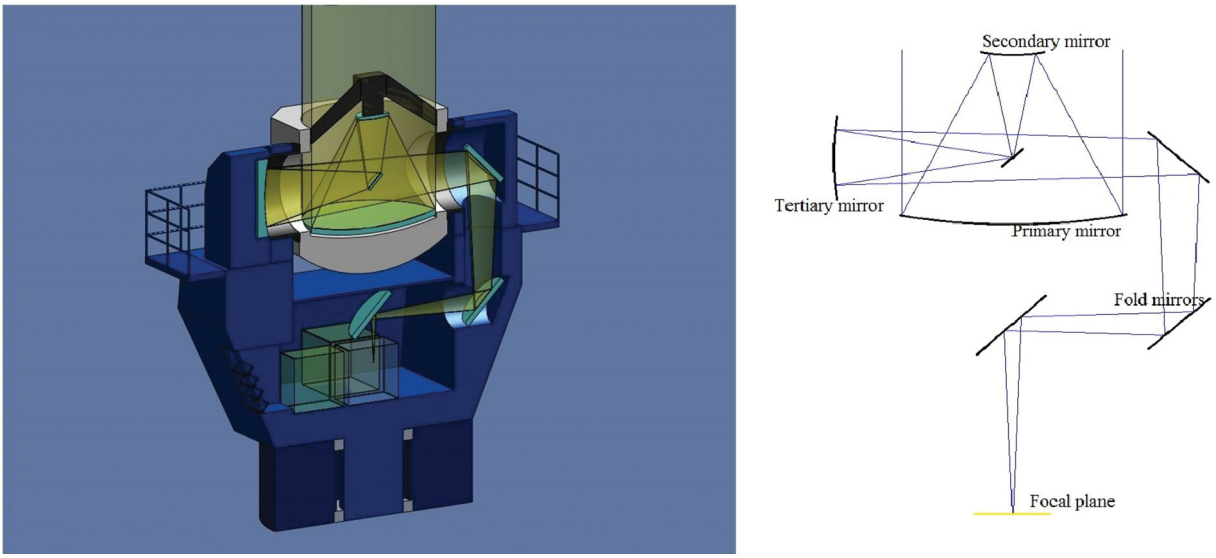

Figure 2. KDUST layout.

model and optical layout are shown in Fig. 2. The required image quality measured by the 80 per cent encircled energy is less than 0.3 arcsec in accordance with the free seeing parameter of Antarctic Dome A. The F/1.06 primary mirror can guarantee a short tube and large back focal length to simplify the arrangement of the focal instruments, and the instruments will remain motionless during pointing or tracking. The main optical parameters of the mirrors are summarized in Table 1. The telescope residual wavefront error is 0.41 λ peak-to-valley (PV) and 0.10 λ root-mean-square (RMS) of the maximum 0°.75 off-axis field of view, while the wavefront error is 0.18 λ PV and 0.05 λ RMS of the on-axis field, as shown in Fig. 3.

3.2 Recording the field aberrations pattern of each d.o.f.

The primary mirror is excluded from the alignment procedure and is set as a datum because the primary pointing direction will establish the optical axis of the telescope. Fold mirror 1, located between the primary and secondary mirrors, has both tilt and linear displacement errors, which are equivalent to misalignment of the tertiary mirror. In this study, we set fold mirror 1 to be fixed and only explore the tertiary misalignment. As determined by sensitivity analysis, the secondary mirror tilt is the most sensitive element, and when the secondary tilts 10 arcsec, it will result in a 3.31 λ PV error in the 0°.75 off-axis field. The same scale error will result from 41.7 μm decentration of the secondary, and either a 30.3-arcsec tilt or a 305-μm decentration of the tertiary. Meanwhile, taking the axial misplaced error into account, a 436-μm misplacement of the secondary or a 78.2-μm misplacement of the tertiary will bring about 3.31 λ PV wavefront error. Each d.o.f. is individually perturbed by the unit value listed for the corresponding d.o.f. in Table 2, and each

Table 1. Main optical design parameters for KDUST.

Element	Radius (mm)	Clear aperture (mm)	Conic constant	Surface type
Primary	− 5005.4	2500	− 0.966	Standard
Secondary	− 2058.0	610	− 7.101	Standard
Tertiary	3600.0	1350	− 0.527	Even Asphere

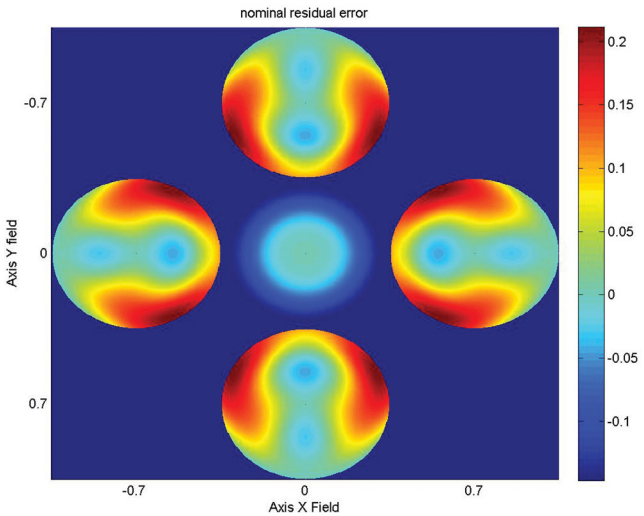

Figure 3. Residual wavefront error of five fields.

d.o.f. perturbation generates different field aberration patterns but with a wavefront error on the same scale. The analysis will improve the calculations of the misalignments. The primary concern of the unit-value selection is that the size of the unit value for each d.o.f. will directly reveal the sensitivity.

After modelling the system in ZEMAX, each d.o.f. is perturbed by the unit value, and the field aberrations are recorded. The field-dependent aberrations introduced by each d.o.f.'s perturbation are given in Fig. 4. The five fields are the on-axis field and the four

Table 2. KDUST d.o.f. for alignment.

Number	Degrees of freedom	Unit value
1,2	Secondary *X* and *Y* decentre (μm)	41.7
3,4	Secondary *X* and *Y* tilt (arcsec)	10
5	Secondary axial position (μm)	436
6,7	Tertiary *X* and *Y* decentre (μm)	305
8,9	Tertiary *X* and *Y* tilt (arcsec)	30.3
10	Tertiary axial position (μm)	78.2

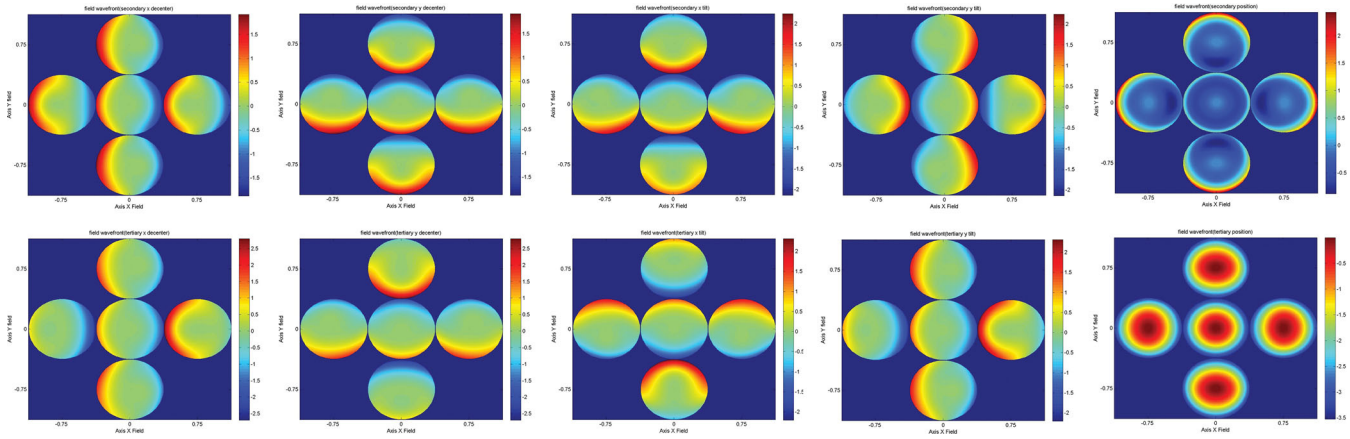

Figure 4. Field wavefront maps of each d.o.f. perturbation. The upper figures are for d.o.f. 1−5, while the lower figures are d.o.f. 6−10.

Table 3. Values of orthogonal DZPs for Z4 and Z11.

DZP terms	Secondary position	Tertiary position
$Z1_{\text{field}} \times Z_4$	0.0285	− 0.0968
$Z1_{\text{field}} \times Z_{11}$	0.0259	0.0004

off-axis fields, which are each off-axis along the *X* or *Y* axes by 0.°75. We conclude that d.o.f.5 and d.o.f.10 must be treated differently with the Zernike terms Z4 and Z11, respectively. Meanwhile, the other eight d.o.f. perturbations produce the same field-dependent aberration patterns, which primarily indicate that the astigmatism and coma can be decomposed into Z5 and Z6 and into Z7 and Z8, respectively.

The field aberration patterns of each d.o.f. can be numerically described by DZP coefficients. The misaligned field aberrations of the axial positions of the secondary and tertiary mirrors are described with Z4 and Z11 orthogonal DZP terms, as summarized in Table 3. Meanwhile, the decentre and tilt misaligned field aberrations are described with the DZP terms Z5, Z6, Z7 and Z8 listed in Table 4. The orthogonal DZP terms, which are used in the unit matrix, are selected according to their linear dependence on the misalignment. There are more linear terms because the combinations of field Zernike polynomials and pupil Zernike polynomials vary based on the DZP equation derived by Manuel (2009). However, 10 terms are sufficient for calculating the 10 d.o.f., and can deliver a suitable solution for misalignment. Moreover, additional linear terms will not improve the result but will cause fluctuations of less sensitive d.o.f., such as the tertiary decentre.

Table 5. Values of orthogonal DZPs values for the misaligned aberrations.

DZP terms	Aberration coefficients ($\times 10^{-3}$)
$Z1_{\text{field}} \times Z_4$	− 1432.5
$Z1_{\text{field}} \times Z_{11}$	318.2
$Z2_{\text{field}} \times Z_5 + Z3_{\text{field}} \times Z_6$	− 1.1
$Z2_{\text{field}} \times Z_5 - Z3_{\text{field}} \times Z_6$	949.4
$Z3_{\text{field}} \times Z_5 + Z2_{\text{field}} \times Z_6$	− 839.9
$Z3_{\text{field}} \times Z_5 - Z2_{\text{field}} \times Z_6$	0.31
$Z1_{\text{field}} \times Z_7$	− 1760.3
$Z2_{\text{field}} \times Z_8$	− 270.9
$Z4_{\text{field}} \times Z_7$	− 1827.0
$Z4_{\text{field}} \times Z_8$	− 281.5

3.3 Calculation of the KDUST misalignment

Normally, measuring implements, which are used for aligning telescopes, can easily guarantee an accuracy of 0.1 mm and 10 arcsec. More advanced methods or more sophisticated devices, which are time-consuming and expensive, are required for alignment with higher accuracy. When exploring the alignment metrology of KDUST, a misaligned optical system is modelled by ZEMAX software. The values of DZPs for the misaligned aberrations are shown in Table 5. The hypothetical misalignment values are shown in Table 6.

The 10 d.o.f. are separated into two axially misplaced d.o.f. and eight decentre or tilt d.o.f., and the processed results are listed in Table 6. The misalignment solutions are accurate, including the less sensitive d.o.f., such as the decentre of the tertiary mirror. The residual wavefront errors of the alignment simulation are 0.39 λ PV

Table 4. Values of orthogonal DZPs for Z5, Z6, Z7 and Z8.

	Degrees of freedom, unit ($\times 10^{-3}$)							
DZP terms	1	2	3	4	6	7	8	9
$Z2_{\text{field}} \times Z_5 + Z3_{\text{field}} \times Z_6$	0	− 0.013	− 0.022	0	0	− 0.041	0.029	0
$Z2_{\text{field}} \times Z_5 - Z3_{\text{field}} \times Z_6$	0	2.0	20.6	0	0	11.5	5.6	0
$Z3_{\text{field}} \times Z_5 + Z2_{\text{field}} \times Z_6$	2	0	0	20.6	11.5	0	0	5.6
$Z3_{\text{field}} \times Z_5 - Z2_{\text{field}} \times Z_6$	− 0.013	0	0	0.022	− 0.041	0	0	− 0.029
$Z1_{\text{field}} \times Z_7$	0	− 19.8	− 19.7	0	0	− 20.0	18.9	0
$Z2_{\text{field}} \times Z_8$	− 19.8	0	0	19.7	− 20.0	0	0	18.9
$Z4_{\text{field}} \times Z_7$	0	− 20.5	− 20.4	0	0	− 20.8	19.7	0
$Z4_{\text{field}} \times Z_8$	− 20.5	0	0	20.4	− 20.8	0	0	− 19.7

Table 6. Hypothetical misalignments and corresponding solutions.

Degrees of freedom	Misaligned value	Unit value	Solution
	Secondary mirror		
X decentre (μm)	126	41.7	126.32
Y decentre (μm)	336	41.7	337.33
X tilt (arcsec)	28	10	27.95
Y tilt (arcsec)	42	10	42.06
Axial position (μm)	523	436	522.98
	Tertiary mirror		
X decentre (μm)	201	305	201.25
Y decentre (μm)	163	305	161.33
X tilt (arcsec)	79	30.3	79.04
Y tilt (arcsec)	59	30.3	58.82
Axial position (μm)	145	78.2	143.55

and 0.09 λ RMS of the maximum field and 0.28 λ PV and 0.07 λ RMS of the on-axis field, which are quantities so small that we can hardly discern these deviations from the nominal design.

When the telescope is aligned in the workshop, the explicit solution will ensure a fully aligned state. Therefore, we can eliminate the less sensitive d.o.f., such as the tertiary decentre, using mechanical methods. Then, the *in situ* assembly or alignment may be efficient, and only two fields of wavefront measurement will be sufficient. Moreover, the secondary mirror should be selected as an active compensator for maintaining the alignment as well as for primary mirror figure errors, especially the low-order coma figure error.

3.4 Calculation of the KDUST primary mirror figure error

While calculating the correction for the misalignment, the DZPs from Z4 to Z8 and Z11 are used. When the tertiary mirror's d.o.f. are eliminated, the DZP matrix offers an opportunity for calculating the primary mirror figure error because the low-order figure error can also be treated as a d.o.f. For instance, the field aberration pattern of comatic figure error is similar to that of a tilt or decentre of the secondary. Meanwhile, note that the constant Z5 and Z6 DZP terms are not used in the alignment procedure because they are not linearly dependent on the misalignment; however, they are linearly dependent on the astigmatic figure error of the primary.

As in the alignment procedure described in Section 3.3, we model the nominal system (modified by shop testing results) including the effect of figure error and we set the unit coefficient value of Z4 to 3.12×10^{-4} Z4, those of Z5 and Z6 to 2.275×10^{-4} and those of Z7 and Z8 to 6.36×10^{-5}. Each unit perturbation value will cause a 3.31 λ PV wavefront error, which is the same as the unit misalignment perturbation. The field aberration patterns are numerically characterized by the DZP matrix with $Z1_{\text{field}} \times Z_5$ and $Z1_{\text{field}} \times Z_6$ terms attached. The field aberration patterns are illustrated in Fig. 5, with unit misalignment of the secondary and unit perturbation of the primary mirror figure error. Then, a real system is modelled with the hypothetical misaligned values listed in Table 7. The calculated value of the secondary mirror misalignments and primary mirror figure errors coincide with the hypothetical values. The residual aberrations are compensated, resulting in the achievement of full alignment, although the correction is so small that the difference from nominal design can hardly be discerned.

In a misaligned optical system, the low-order astigmatic figure errors as well as misalignment can be accurately measured (Fuerschbach, Rolland & Thompson 2012). However, the solutions of low-order comatic figure errors are not accurate. These errors are compensated by misalignments, as Table 7 shows. In this case, comatic figure error is related to the decentre of the secondary mirror (Thompson 2013).

4 CONCLUSION

We have developed a modified alignment metrology and we have numerically simulated the alignment procedure using the current optical model of KDUST. The metrology, which is based on field-dependent aberration measurement and decomposition, can be applied to accurately calculate multi-element misalignments as well as low-order figure errors. For real applications, we believe that a portable interferometer, which incorporates a tip−tilt flat mirror, can be used for quality alignment. The sensitivity analysis indicates that the secondary mirror is the most sensitive element, and therefore an active supported secondary mirror should be used as an effective compensator for misaligned states. Furthermore, active optics are needed for KDUST in order to ensure good image quality in the harsh Antarctic environment. The alignment metrology introduced in this study can be applied in the sensing and correction of low-order figure errors in active optics. Because Dome A is an unattended astronomical site, it will be of great help to use wavefront sensors at the specified fields because this would enable the monitoring and maintaining of the telescope alignment status in real time.

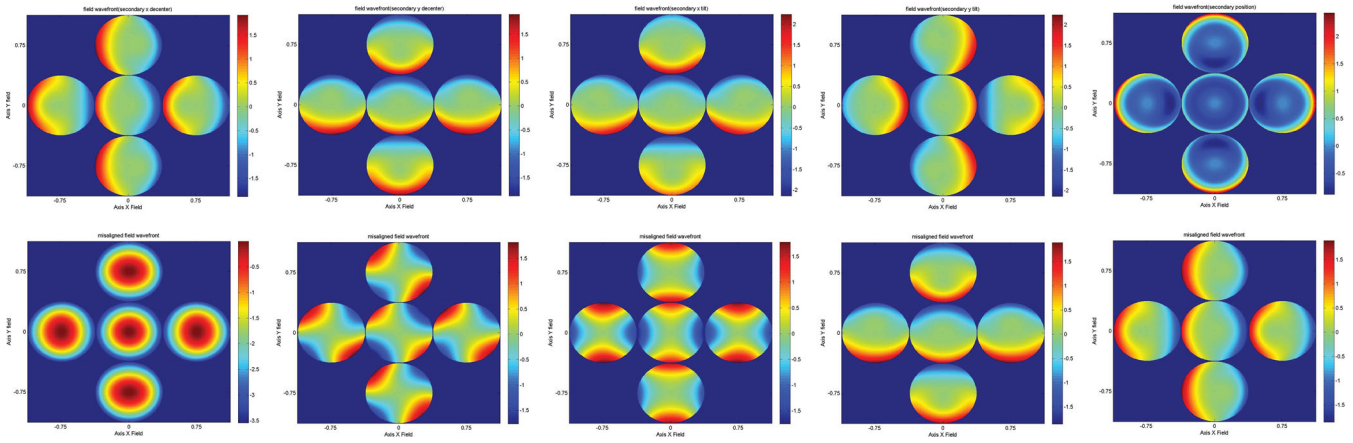

Figure 5. Field wavefront maps for each d.o.f. perturbation. The upper figures are for the d.o.f. of the secondary mirror, while the lower figures are the figure errors from Z4 to Z8.

Table 7. Hypothetical misalignment and figure errors values and corresponding solutions.

Degrees of freedom	Perturb. value	Unit value	Solution
Secondary mirror			
X decentre (μm)	154	41.7	159.30
Y decentre (μm)	38	41.7	44.35
X tilt (arcsec)	45	10	44.84
Y tilt (arcsec)	23	10	23.12
Axial position (μm)	235	436	234.73
Primary mirror (coefficient units 10^{-4})			
Defocus Z4	5	3.12	5.01
Astigmatism Z5	6	2.275	5.99
Astigmatism Z6	3	2.275	2.98
Coma Z7	0.2	0.636	0.14
Coma Z8	1.1	0.636	1.03

ACKNOWLEDGEMENTS

We would like thank Dr Bai Hua for useful discussions and suggestions for the calculation. We are grateful for the support of the National Natural Science Fund of China (11190011) and the National Key Basic Research Programme of China (973 Programme 2013CB834901).

REFERENCES

Buchroeder R. A., 1976, PhD, University of Arizona
Fuerschbach K., Rolland J. P., Thompson K. P., 2012, Optics Express, 20, 20139
Hopkins H. H., 1950, Wave Theory of Aberrations. Clarendon Press, Oxford
Manuel A. M., 2009, PhD, University of Arizona
Mcleod B. A., 1996, PASP, 108, 217
Sebag J., Gressler W., Schmid T., Rolland J. P., Thompson K. P., 2012, PASP, 124, 380
Shack R. V., Thompson K. P., 1980, Proc. SPIE, 251, 146
Thompson K. P., 2005, Optical Society of America Journal, 22, 1389
Thompson K. P., 2013, Advances Optical Technology, 2, 89
Thompson K. P., Fuerschbach K., Schmid T., Rolland J. P., 2009, Proc. SPIE, 7433, 74330B
Thompson K. P., Schmid T., Rolland J. P., 2008, Optics Express, 16, 20345
Yang H. et al., 2010, PASP, 122, 490
Zhengyang L., Xiangyan Y., Xiangqun C., 2012, Proc. SPIE, 8444, 8444

This paper has been typeset from a TEX/LATEX file prepared by the author.